Squeezing in the Audio Gravitational-Wave Detection Band

Kirk McKenzie,[1] Nicolai Grosse,[1,2] Warwick P. Bowen,[2] Stanley E. Whitcomb,[3] Malcolm B. Gray,[1]
David E. McClelland,[1] and Ping Koy Lam[1,2]

[1]*Center for Gravitational Physics, Department of Physics, Faculty of Science, The Australian National University, ACT 0200, Australia*

[2]*Quantum Optics Group, Department of Physics, Faculty of Science, The Australian National University, ACT 0200, Australia*

[3]*LIGO Laboratory, California Institute of Technology, Pasadena, California, 91125, USA*

(Received 21 May 2004; published 15 October 2004)

We demonstrate the generation of broadband continuous-wave optical squeezing from 280 Hz–100 kHz using a below-threshold optical parametric oscillator (OPO). The squeezed state phase was controlled using a noise locking technique. We show that low frequency noise sources, such as seed noise, pump noise, and detuning fluctuations, present in optical parametric amplifiers, have negligible effect on squeezing produced by a below-threshold OPO. This low frequency squeezing is ideal for improving the sensitivity of audio frequency measuring devices such as gravitational-wave detectors.

DOI: 10.1103/PhysRevLett.93.161105 PACS numbers: 04.80.Nn, 42.50.Lc, 42.65.Yj, 95.55.Ym

Squeezed light was proposed for quantum noise reduction in interferometric gravitational-wave (GW) detection over two decades ago [1]. Since then, the first generation of long baseline GW detectors—LIGO [2], VIRGO [3], GEO 600 [4], and TAMA 300 [5]—have been built and recently begun operation. The second generation of detectors, such as Advanced LIGO [6], are currently in the late planning stages. The prediction that they will be quantum noise limited (QNL) across most of the GW signal band (10–10^4 Hz) has led to further theoretical investigations into the use of squeezing [7–9] and other optical methods [10–12] for quantum noise reduction. However, to date only one experimental demonstration of quantum noise reduction in a GW detector configuration has been reported [13], and that result was obtained well above the GW signal band.

To be applicable to GW detectors, the requirements on squeezing include continuous-wave (CW) at 1064 nm, squeezed at the GW signal frequency, compatible with readout techniques [14], controllable phase, and a high level of squeezing. Although squeezed light was first demonstrated in 1985 [15], a CW squeezed source at audio frequencies has not been reported until now. Laser relaxation oscillation and other technical noise sources have typically confined squeezing to the MHz range.

Two of the most successful systems for squeezed state generation have been the optical parametric oscillator (OPO) and optical parametric amplifier (OPA), for example, see [16,17]. OPA and OPO have the same underlying second order nonlinearity, however, they differ in that the OPA process has a coherent seed field at the fundamental wavelength, whereas the OPO does not and is seeded only by vacuum fluctuations. In theory OPO/OPA systems can produce squeezed states that fulfill the GW detector requirements outlined above. Experiments to date have been able to demonstrate each requirement, except squeezing in the GW signal band. The lowest frequency CW squeezing experiments reported so far include Bowen *et al.* [18], Schnabel *et al.* [19], and Laurat *et al.* [20] demonstrating squeezing down to 220, 80, and 50 kHz, respectively. These experiments used either OPO or OPA, with [18,19] relying on common mode noise cancellation techniques.

In this Letter we report the generation of high purity broadband squeezing by a below-threshold OPO at sideband frequencies from 280 Hz to well above 100 kHz, covering a large portion of the audio GW detection band. The phase of the squeezed vacuum relative to the homodyne detector was controlled without a carrier by using a noise dither locking technique; see for example [20]. The inferred squeezing level measured at 11.2 kHz (adjusted for detection efficiency) at the OPO output was 5.5 ± 0.6 dB below the shot noise limit (SNL) with inferred purity of 1.3 ± 0.1, close to a minimum uncertainty state. We compare OPO and OPA operation and find that the presence of a coherent seed field leads to dramatic degradation of the squeezing at low frequency, due to technical noise coupling. The system operating as an OPO displays immunity to the same technical noise that degrades OPA squeezing.

Amplitude (+) and phase (−) quadrature variances, $V^{\pm}_{\mathrm{sqz}} = \langle (X^{\pm}_{\mathrm{sqz}})^2 \rangle$, at the output of the singly resonant OPO/OPA on resonance can be modeled using linearized formalism by

$$V^{\pm}_{\mathrm{sqz}}(\omega) = \{C_s V^{\pm}_s(\omega) + C_l V^{\pm}_l(\omega) + C^{\pm}_v(\omega) V^{\pm}_v(\omega) + \alpha^2 [C_p V^{\pm}_p(\omega) + C^{\pm}_{\Delta} V_{\Delta}(\omega)]\}/|D^{\pm}(\omega)|^2, \quad (1)$$

where $V^{\pm}_{\mathrm{sqz}}$ contains contributions from the seed field, $V^{\pm}_s$, the pump field, $V^{\pm}_p$, vacuum fluctuations from intracavity loss, $V^{\pm}_l$, vacuum fluctuation entering through the output coupler, $V^{\pm}_v$, and noise due to detuning fluctuations in the cavity [21], V_{Δ}, which arise from acoustomechanical disturbances. Other sources, such as phase matching fluctuations, are not discussed here. The denominator and coupling coefficients are given by [22,23]

$$D^{\pm}(\omega) = i\omega + \kappa_a + \begin{bmatrix} 3 \\ 1 \end{bmatrix} \epsilon^2\alpha^2/(2\kappa_b) \mp \epsilon\beta,$$

$$C_s = 4\kappa^a_{\rm in}\kappa^a_{\rm out}, \qquad C_l = 4\kappa^a_l\kappa^a_{\rm out},$$

$$C^{\pm}_v(\omega) = |2\kappa^a_{\rm out} - D^{\pm}(\omega)|^2, \qquad C_p = 4\kappa^a_{\rm out}\kappa^b_{\rm in}(\epsilon/\kappa_b)^2,$$

$$C^{\pm}_{\Delta} = 8\kappa^a_{\rm out}\begin{bmatrix} 0 \\ 1 \end{bmatrix},$$

where the intracavity fundamental field, $\alpha = \sqrt{n}$, with n the mean intracavity photon number. The parameters $\kappa^a_{\rm out}$, $\kappa^a_{\rm in}$, and κ^a_l are the decay rates of α due to the output coupler, input coupler, and loss, respectively. $\kappa^b_{\rm in}$ is the decay rate of the intracavity second harmonic field, β, due to the input coupler. κ_a and κ_b are the total decay rates for α and β. ϵ is the nonlinear coupling parameter and ω is a small frequency shift relative to the carrier frequency. The first three terms in Eq. (1) are standard contributions from the seed noise entering through the input coupler, vacuum fluctuations due to intracavity loss, and vacuum fluctuations entering through the output coupler. The last two terms scale with α^2 and show an important difference between OPO and OPA operation. That is, the fluctuations of the pump, $V^{\pm}_p$, and detuning, V_{Δ}, are coupled into the squeezed field, $V^{\pm}_{\rm sqz}$ via the beat with the intracavity fundamental field, α. Thus, a below-threshold OPO ($\alpha = 0$) should be immune to these two noise sources to first order.

A schematic of the experiment setup is in Fig. 1. A Nd:YAG laser operating at 1064 nm was split into two beams. One beam is used to pump the second harmonic generator (SHG). The other was spatially and temporally filtered by a mode-cleaner cavity [24] and used as the seed beam for the OPA and as local oscillator (LO) for the homodyne detector. The OPO/OPA and SHG are constructed out of type-I phase-matched MgO : $LiNbO_3$ hemilithic crystals. The curved surface of these crystals were coated for high reflectivity (HR) and the flat surface coated for antireflectivity (AR) at both 532 and 1064 nm. In both the SHG and OPO/OPA, standing-wave cavities were formed at 1064 nm between the HR surface of the crystal together with an external mirror of reflectivity $R_{\rm IR} = 96\%$ at 1064 nm and $R_{\rm GR} < 4\%$ at 532 nm. The OPO/OPA was pumped with 100 mW of 532 nm light which double passed through the crystal giving a measured classical gain of 5. Results were taken in the OPO mode, and in the OPA mode while varying the seed power from 1 nW–6 μW. The squeezed state was detected on the homodyne detection system which had 96.5% fringe visibility. While in the OPO operation, a Faraday isolator was inserted between the OPO cavity and the photodetectors to reduce LO backscattered light. The photodetectors were built around ETX 500 photodiodes with 93% quantum efficiency. The common mode rejection of the homodyne detector was over 55 dB.

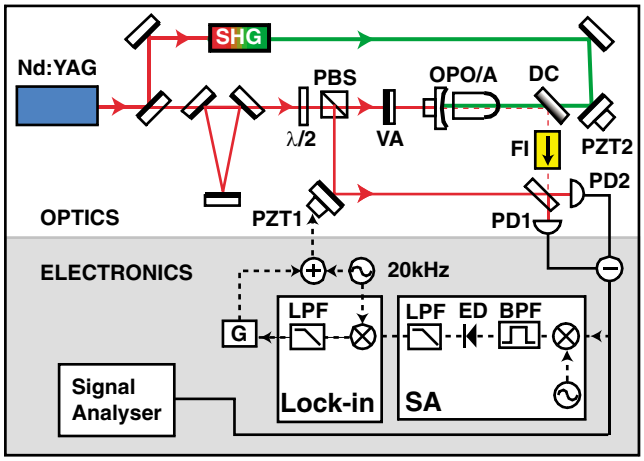

FIG. 1 (color online). Schematic of the experiment. The experiment was operated in both OPO and OPA modes. The OPA seed power was varied using a variable attenuator (VA). The OPO cavity was isolated from backscatter off the photodetectors using a Faraday isolator (FI). The control electronics for the homodyne detection phase are indicated by dashed lines. SA, spectrum analyzer; BPF, band pass filter; ED, envelope detector; LPF, low pass filter; G gain stage; SHG, second harmonic generator; OPO/A-optical parametric oscillator/amplifier; PZT, piezoelectric transducer; PBS, polarizing beamsplitter; $\lambda/2$-half-wave plate; DC, dichroic mirror; PD, photodetector.

The control electronics for the homodyne detection phase are indicated by dashed lines in Fig. 1. This error signal was generated by dithering the LO phase and demodulating the difference photocurrent noise power. The noise power was detected using a spectrum analyzer (Agilent-E4407B, zero span at 2 MHz, resolution bandwidth (RBW) = 300 kHz, video bandwidth (VBW) = 30 kHz) then demodulated with a lock-in amplifier [Stanford Research Systems (SRS)-SR830] and filtered before being fed back to PZT1. The stability of the homodyne detection phase enabled us to take results without locking the OPO/OPA cavity, which typically stayed on resonance for 10 sec. All data, except that in Fig. 3, were recorded on a dynamic signal analyzer (SRS-SR785).

The OPO squeezing spectrum from 100 Hz–100 kHz is shown in Fig. 2 [25]. Trace (a) shows the quantum noise limit of the homodyne detection system. The measurement of the squeezed light is shown in trace (b). Trace (c) shows the electronics noise of the detection system. The roll-up in noise power in traces (a) and (b) is attributable to the imperfect homodyne cancellation at low frequencies. We see that broadband squeezing is obtained from 280 Hz to 100 kHz, with the exception of a locking signal peak at 20 kHz. Squeezing could not be measured at 150 and 250 Hz due to power supply harmonics in the electronic noise.

Figure 3 shows the OPO squeezed state at 11.2 kHz as the homodyne phase was varied. The measured squeezed state purity is $V^+V^- = 1.6 \pm 0.2$. The squeezing and purity at the output of the OPO can be inferred by taking into account the photodetection and homodyne efficien-

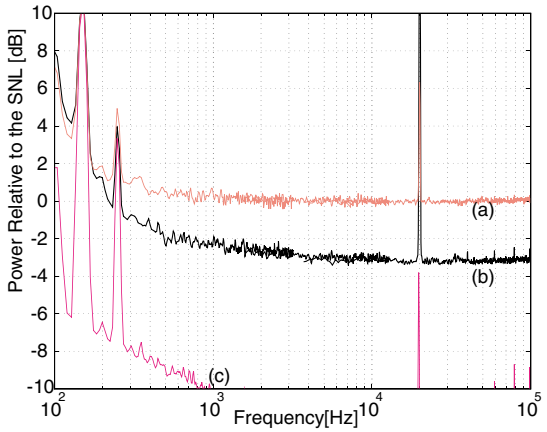

FIG. 2 (color online). Measured noise spectra for (*a*) the quantum noise limit, (*b*) the squeezed light, and (*c*) the electronic noise of the homodyne detection system. The traces are pieced together from three FFT frequency windows: 100 Hz–3.2 kHz, 1.6 kHz–12.8 kHz, and 3.8 kHz–100 kHz. Each point is the averaged rms value of 500, 1000, and 2000 measurements made in the respective ranges. The RBW of the three windows was 8, 32, and 128 Hz, respectively. The electronic noise was −12 dB below the quantum noise from 10–100 kHz. The 20 kHz peak arises from the homodyne locking signal. Peaks at 50 Hz harmonics are due to electrical mains supply.

cies and optics loss. The inferred purity is $V^+V^- = 1.3 \pm 0.1$ and the inferred squeezing is $V_{\mathrm{sqz}} = -5.5 \pm 0.6$ dB.

Figure 4 shows a more detailed analysis of the squeezing spectrum at the lowest frequency window of 100 Hz–3.2 kHz. Trace (a) shows the squeezing spectrum obtained without an isolator in front of our homodyne detection system. We observed large peaks between 300 and 700 Hz due to low frequency noise contamination. This contamination is attributed to light from the LO backscattered from the photodetectors feeding into the OPO cavity. We

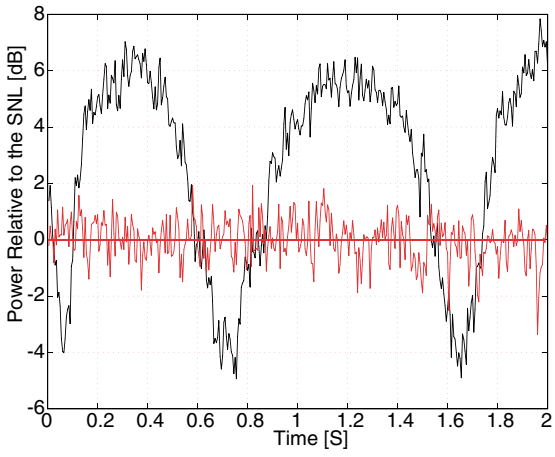

FIG. 3 (color online). The squeezed state at 11.2 kHz as the phase of the homodyne is varied. RBW = 1 kHz, VBW = 30 Hz. Electronic noise (9 dB below SNL) was subtracted from the data.

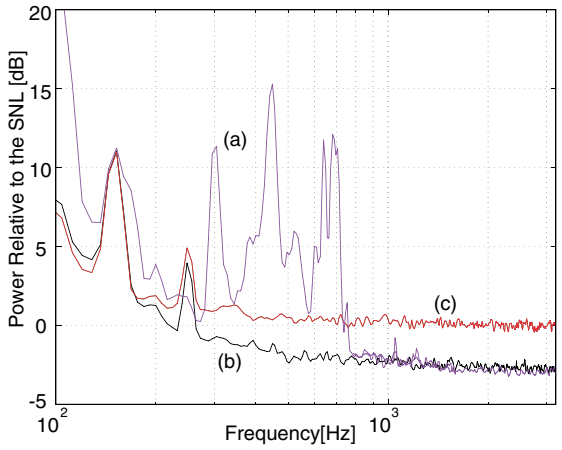

FIG. 4 (color online). The OPO spectrum 100 Hz–3.2 kHz without (a) and with (b) the Faraday isolator between the OPO cavity and homodyne detector. RBW = 8 Hz; number of rms averages for (a) 400 and for (b) and (c) 500. Electronic noise (not shown) was not subtracted.

note that even with the photodetectors tilted away from retroreflection, the scattering from the front face of the detectors, which is estimated to be of the order of 1 pW, is sufficient to seed the crystal and causes parametric amplification. With the Faraday isolator in place noise coupling via parametric amplification is eliminated, as shown by trace (b). The squeezed beam experiences an extra 9% transmission loss through the isolator. Similar to Fig. 2, electronic noise is still present at 150 and 250 Hz.

The OPA spectrum from 2–100 kHz is shown in Fig. 5 for three different seed powers, 1 nW, 700 nW, and 6 μW. The data were recorded for optimal squeezing at 50 kHz. The 1 nW seed power spectrum resembles the OPO spec-

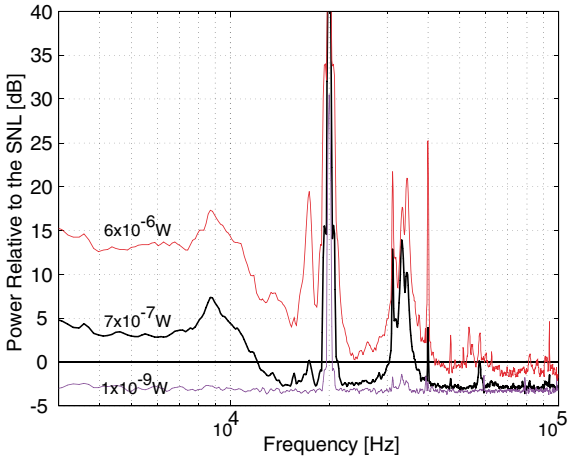

FIG. 5 (color online). The OPA spectrum 2–100 kHz with different OPA seed powers. The variance of the seed beam with power 6 μW was less than 4 dB above the SNL across the spectrum. RBW = 128 Hz. Number of rms averages, 1000, except for 6 μW seed power which had 500 rms averages. Electronic noise (at −12 dB) was subtracted from all traces.

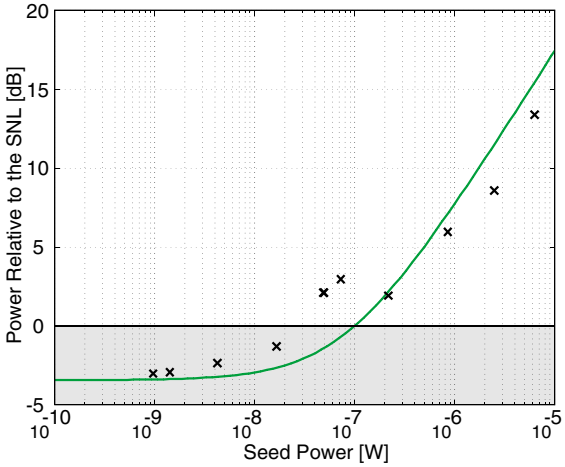

FIG. 6 (color online). The average noise power from 5–6 kHz as a function of seed power, experimental data indicated by "x", model fit given by line. Electronic noise (at −12 dB) was subtracted from all data.

trum, with the exception of one added feature at 34 kHz. The spectrum of the 700 nW seed power shows the feature at 34 kHz has increased in amplitude with additional excess noise at other frequencies thereby limiting squeezing to above 10 kHz. The feature at 8 kHz was also present in the pump intensity noise spectrum and is expected to have coupled into the squeezed field via the intracavity fundamental field. As the seed power was increased further, the noise floor and features in the spectrum continued to increase; by seed power 6 μW there is no longer squeezing below 40 kHz. The noise power increase of the OPA spectrum with seed power is evident in Fig. 6, which shows the mean noise power between 5–6 kHz as a function of seed power. The experimental points indicated by "x" can be compared with a model which has linear dependence on seed power, given by the solid line. Although there are large uncertainties expected in the experimental data, since the OPA cavity was not locked, the data are not inconsistent with the linear trend predicted by the theory in Eq. (1).

In summary, we have presented results demonstrating broadband OPO squeezed vacuum down to 280 Hz. The phase of squeezed vacuum was controlled using a noise locking technique. Such squeezed states could already be of use for reduction of shot noise in first generation GW detectors. The comparison of the OPO and OPA results highlights the immunity of OPO and the sensitivity of OPA to technical noise. The direction of our future research will be to implement an OPO cavity lock, increase the level of squeezing and probe frequencies lower than 100 Hz for use in second generation GW detectors.

In addition to the possible application to GW detectors, low frequency squeezed light could potentially be used to enhance many measurement devices with optical readout. These include atomic force microscopes [26] and thermo-optical spectrometers [27]. Many long-standing experimental goals in quantum optics, such as the inhibition of atomic decay [28] and sub-Doppler cooling of two-level atoms [29], could also be facilitated using broadband low frequency squeezing.

We thank Keisuke Goda, Julien Laurat, and Nicolas Treps for useful discussions. This research was supported by the Australian Research Council. S.W. was supported by the United States National Science Foundation under Cooperative Agreement No. PHY-0107417. This Letter has been assigned LIGO Laboratory document No. LIGO-P040018-00-R.

[1] C. M. Caves, Phys. Rev. D **23**, 1693 (1981).
[2] B. Abbott *et al.*, Nucl. Instrum. Methods **517**, 154 (2004).
[3] B. Caron *et al.*, Classical Quantum Gravity **14**, 1461 (1997).
[4] H. Lück *et al.*, Classical Quantum Gravity **14**, 1471 (1997).
[5] M. Ando *et al.*, Phys. Rev. Lett. **86**, 3950 (2001).
[6] D. Shoemaker, Classical Quantum Gravity **20**, S11 (2003).
[7] H. J. Kimble *et al.*, Phys. Rev. D **65**, 022002 (2002).
[8] J. Harms *et al.*, Phys. Rev. D **68**, 042001 (2003).
[9] T. Corbitt and N. Mavalvala, Proc. SPIE Int. Soc. Opt. Eng. **5111**, 23 (2003).
[10] J.-M. Courty, A. Heidmann, and M. Pinard Phys. Rev. Lett. **90**, 083601 (2003).
[11] A. Buonanno and Y. Chen Phys. Rev. D **64**, 042006 (2001).
[12] V. B. Braginsky *et al.*, Phys. Rev. D **61**, 044002 (2000).
[13] K. McKenzie *et al.*, Phys. Rev. Lett. **88**, 231102 (2002).
[14] A. Buonanno, Y. Chen, and N. Mavalvala, Phys. Rev. D **67**, 122005 (2003).
[15] R. E. Slusher *et al.*, Phys. Rev. Lett. **55**, 2409 (1985).
[16] P. K. Lam *et al.*, J. Opt. B **1**, 469 (1999).
[17] M. Xiao *et al.*, Phys. Rev. Lett. **59**, 278 (1987).
[18] W. P. Bowen *et al.*, J. Opt. B, **4**, 421 (2002).
[19] R. Schnabel *et al.*, Opt. Commun. **240**, 185 (2004).
[20] J. Laurat *et al.*, quant-ph/0403224.
[21] B. C. Buchler *et al.*, Opt. Lett. **24**, 259 (1999).
[22] W. P. Bowen, Ph.D. thesis, Australian National University, Canberra, 2004.
[23] The notation $[^3_1]$ means multiply by 3 for the amplitude quadrature or 1 for the phase quadrature.
[24] A. Rüdiger *et al.*, Opt. Acta **28**, 641 (1981).
[25] The squeezing spectrum continues to tens of MHz, as reported in [22].
[26] N. Treps *et al.*, Science **301**, 940 (2003).
[27] A. C. Boccara, D. Fournier, and J. Badoz, Appl. Phys. Lett. **36**, 130 (1980).
[28] C. W. Gardiner, Phys. Rev. Lett. **56**, 1917 (1986).
[29] Y. Shevy, Phys. Rev. Lett. **64**, 2905 (1990).